Crystal Growth

DOI: 10.1002/ange.201104407

Capillarity Creates Single-Crystal Calcite Nanowires from Amorphous Calcium Carbonate**

*Yi-Yeoun Kim, Nicola B. J. Hetherington, Elizabeth H. Noel, Roland Kröger, John M. Charnock, Hugo K. Christenson, and Fiona C. Meldrum**

Amorphous calcium carbonate (ACC) is now recognized to be a common biomineral.[1] While some organisms produce a stable ACC phase which remains amorphous for extended periods of time, the more interesting phase is arguably transient ACC, which acts as a precursor to calcite and aragonite and crystallizes under biological control.[2] This strategy clearly offers organisms a number of advantages over the traditional ion-by-ion growth process.[3] For example, in supplying a dense precursor phase to the mineralization site slow ion diffusion is avoided and high rates of mineralization can be achieved. Further, a high degree of control over the crystallization process can be achieved by modifying the composition of the ACC with organic and inorganic additives, such that crystallization can be triggered as desired. We have also recently suggested that contact of ACC with water is a critical factor in determining its rate of crystallization.[4] This biogenic mineralization strategy has therefore excited much interest as a route to materials synthesis and ACC has been used to synthesize a range of crystalline structures including fibers and thin films,[5–7] mesoporous single crystals,[8] micropatterned single crystals[9] and rods.[10,11]

Here, we explore the possibility of controlling the crystallization of ACC through limiting contact of the mineral with the bulk solution, and demonstrate that remarkable control over the crystal product can be achieved by using this templating methodology. Precipitation of ACC within the rod-shaped pores of polycarbonate track-etch membranes creates a system where most of the surface of an intramembrane particle is in direct contact with the membrane walls and only the ends are in contact with the solution. Subsequent crystallization then yielded single crystals of calcite with rod-like morphologies and aspect ratios of up to 100. This system, in which calcite single crystals are generated from an ACC precursor particle of identical size and shape, is therefore quite distinct from existing methods of production of $CaCO_3$ fibers.[5,7,12–16] These syntheses operate in bulk solution, by using either microemulsions or polymer additives, and the fibers appear to grow through a continuous process. In performing the current experiments, we employ and contrast two methods of preparing ACC and use either low temperature (4 °C) to extend the lifetime of the ACC or the additives poly(acrylic acid) (PAA) or poly(aspartic acid) (PAsp) to generate ACC through a "PILP" (polymer-induced liquid precursor) phase.[1] When calcium carbonate is precipitated in the presence of PAA or PAsp it forms an amorphous, hydrated, polymer-rich phase which displays some fascinating properties and has been termed "PILP" due to the observation that it shows some behavior characteristic of liquids, including the ability to infiltrate into small pores.[17] This PILP phase transforms to ACC in solution over time, which subsequently crystallizes. The current experiments therefore also enable us to investigate the mechanism of infiltration of PILP into porous media and provide strong evidence for capillary action.

ACC was precipitated within "50 nm" and "200 nm" diameter pores of polycarbonate track-etch membranes (where it should be noted that these values represent the pore diameter at the membrane surface such that the average width of the "50 nm" pores was ca. 100 nm and the 200 nm pores ca. 250 nm). In the absence of additives, this was achieved by using an established double-diffusion method,[10,11] where the membrane was placed between two U-tube arms containing high concentrations (0.1M) of $CaCl_2$ and Na_2CO_3, respectively. Performing the experiment at this high supersaturation and low temperature (4 °C) results in the precipitation of ACC in the membrane pores, where the ACC is stable for 25–30 min prior to crystallization. While approximately 50% of the 200 nm pores were filled,[10,11] $CaCO_3$ precipitation only occurred in about 10% of the 50 nm membrane pores, yielding rod-shaped particles with aspect ratios of 10–25 (Supporting Information, Figure SI1). These estimates were made through SEM analysis of intact membranes after crystallization, where the percentages of pores containing particles were evaluated. Electron diffraction showed that they were single crystals of calcite, despite having a granular structure as viewed by TEM (Figure SI1,

[*] Y.-Y. Kim, N. B. J. Hetherington, E. H. Noel, Prof. F. C. Meldrum
School of Chemistry, University of Leeds, Leeds, LS2 9JT (UK)
E-mail: f.meldrum@leeds.ac.uk
Homepage: http://www1.chem.leeds.ac.uk/FCM/
Dr. R. Kröger
Department of Physics, University of York, York, YO10 5DD (UK)
Dr. J. M. Charnock
School of Atmospheric and Environmental Sciences
University of Manchester, Manchester, M13 9PL (UK)
Dr. H. K. Christenson
School of Physics and Astronomy
University of Leeds, Leeds, LS2 9JT (UK)

[**] We thank the EPSRC for financial support via grant EP/E037364/2 (Y.Y.K.) and a DTA award (EPSRC and Unilever) for N.B.J.H. We would also like to thank Dr. Tim Senden (Department of Applied Maths, RSPhysSE, ANU, Canberra) and Dr. Frederik Berthold (Innventia, Stockholm), for useful discussion. We also thank DESY for the provision of beam-time, Edmund Welter on the A1 HASYLAB beam-line, and the EC for financial support. We acknowledge the York JEOL Nanocentre for access to facilities.

Supporting information for this article is available on the WWW under http://dx.doi.org/10.1002/anie.201104407.

inset). These results contrast with the precipitation of $CaCO_3$ in the absence of an ACC precursor phase, where precipitation in the pores is limited. A low yield of misshapen particles is produced in the 200 nm pores,[10] while little precipitation occurs in the 50 nm pores.

Precipitation of ACC in the presence of PAA, which produces a PILP phase, resulted in a marked increase in the yield of intra-membrane particles, and the vast majority of both the 50 nm and 200 nm pores now supported particle formation (Figure 1 a). This was true for experiments carried out by using both the double diffusion method, and by immersing the membrane in 10 mM $CaCl_2$ solution with PAA followed by exposure to ammonium carbonate vapor. The intra-membrane particles formed were again solid, and remarkably, most displayed extremely high aspect ratios as defined by complete filling of the membrane pores. Therefore, calcite nanowires with aspect ratios of ca. 100 were produced in the 50 nm pores (Figure 1 b,c and Figure 2 a). In viewing these images it should be noted that these nanowires often fracture during sample preparation due to the sonication and centrifugation processes used to isolate them from the membrane. That the $CaCO_3$ particles do typically span the entire 10–15 μm thickness of the membranes is clearly seen on imaging bundles of particles generated on incomplete dissolution of the membrane (Figure 1 a shows bundles precipitated in 200 nm membrane pores). Extensive washing then results in separation of the individual rods. The collected

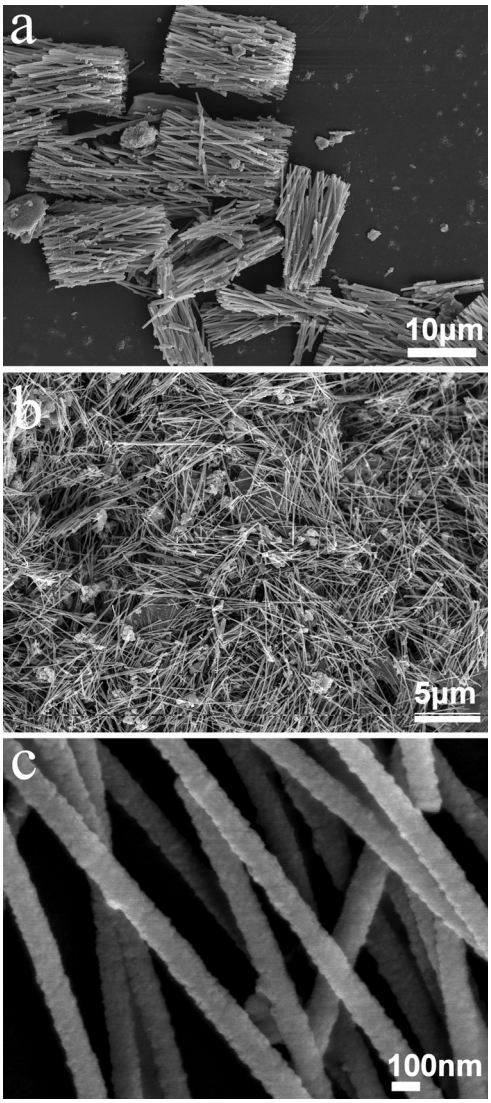

Figure 1. SEM images of calcite particles precipitated in the pores of track etch membranes in the presence of 10 μg mL^{-1} PAA from a PILP precursor phase. The images shown correspond to pore sizes of a) 200 nm and b,c) 50 nm. The pore size quoted is that stated by the manufacturer, and describes the diameter of the pore on the top membrane surface. In reality, the pores are not uniform in width and the average width of the "50 nm" is ca. 100 nm.

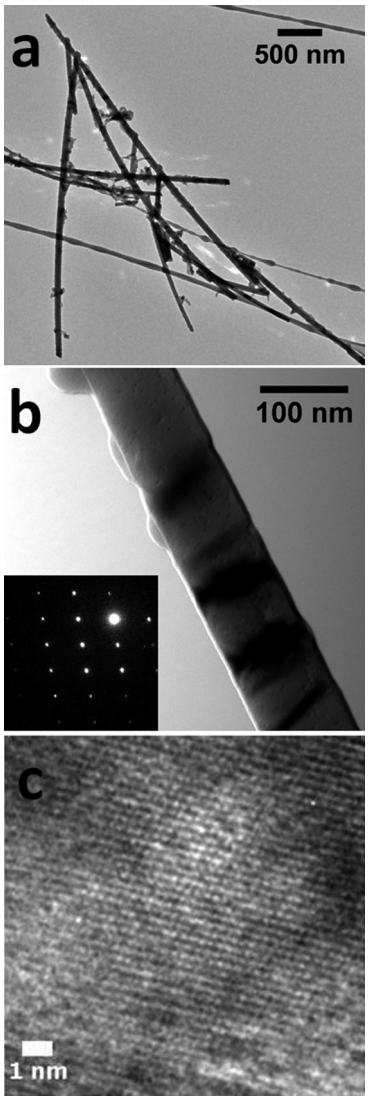

Figure 2. High aspect ratio calcite rods precipitated in 50 nm membrane pores in the presence of 10 μg mL^{-1} PAA. a,b) Bright-field TEM images of the nanorods, with (b) showing a single rod and its corresponding SAED pattern taken close to the [5,1,1] zone axis. c) HRTEM lattice image of a nanorod demonstrating continuity of the crystal lattice. Again, the additional diffuse material is residual polymer from dissolution of the membrane.

nanowires were confirmed as calcite using Raman microscopy and IR spectroscopy (Figure SI2).

The structure of the high aspect ratio rods precipitated in the 50 nm pores using the PILP method was investigated using TEM, high resolution (HRTEM), and selected area electron diffraction (SAED). Electron diffraction demonstrated that the great majority of rods were single crystals of calcite, as judged by carrying out SAED analysis along the entire length of a rod (Figure 2b, inset). A few polycrystalline rods were also sometimes observed. That the rods were single crystals of calcite was supported by HRTEM, and fast-Fourier transformation (FFT) of the lattice images, which showed full continuity in the crystal lattice in all areas examined (Figure 2c and Figure SI3). It is also worth drawing attention to the contrast variation observed in the TEM images which can be attributed to surface irregularities on the rods (as viewed by SEM, Figure 1).[18] No evidence for a nanoparticulate microstructure was obtained.

That confinement of ACC within the membrane pores affects not only the crystal product but the rate of crystallization was also demonstrated using a number of methods. $CaCO_3$ films deposited at the base of the reaction vessel from a solution containing 10 $\mu g\,mL^{-1}$ PAA showed significant crystallinity after 3 h (as judged by polarisation optical microscopy, Figure SI4), a result which was supported by Raman analysis (Figure SI5). In contrast, it was very difficult to isolate rods produced using PILP from the membrane pores after this time, suggesting that they were still amorphous and therefore mechanically unstable. X-ray absorption spectroscopy (XAS) was also used to compare the rates of crystallization in the bulk solution and within the membrane pores, and demonstrated some differences in the crystallization mechanism. Intra-membrane particles produced in 200 nm pores using the PILP method were isolated after 5 h and 12 h, and were compared with ACC produced in bulk solution after the same time periods. Previous analysis of the crystallization of additive-free ACC in membrane pores had shown that this occurs more slowly in the pores than in bulk solution.[10,11] Examination of the pre-edge and XANES regions of the spectra from 5 h samples clearly showed that the material in the bulk solution had a significant degree of crystallinity, while the particles confined within the membrane were still amorphous after this time (Figure 3). The absorption edge of the bulk/control sample comprised two peaks (at 4049.6 eV and 4097 eV), and a shoulder was observed at 4045.8 eV which has been attributed to a 1s–4s transition.[19] These features are unique to the crystalline polymorphs of calcium carbonate.[19,20] In contrast, the membrane sample showed only a single, large peak at the top of the absorption edge at 4050.5 eV, and a pre-edge peak at 4040.6 eV which derives from 1s–3d type transitions.[21] Such a featureless spectrum is again characteristic of ACC.[19–21] The XANES data also clearly showed that crystallisation of the intra-membrane particles occurred on continued incubation of the membrane in solution, and the spectra obtained from 12 h particles displayed the characteristic features of the crystalline polymorphs (Figure 3).

The EXAFS regions of the data were also analyzed, although the structural information obtained from these was

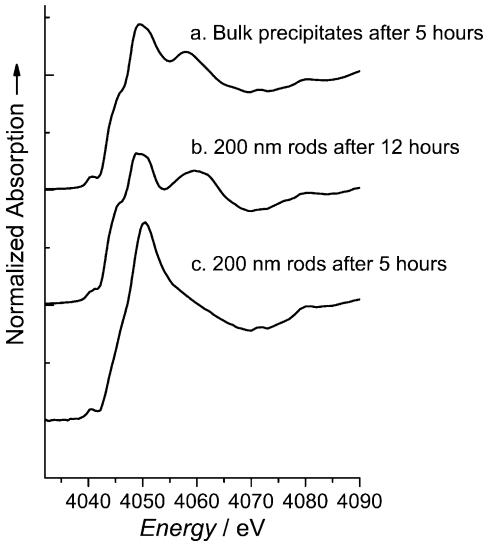

Figure 3. X-ray absorption spectra showing pre-edge and XANES regions of ACC precipitated in the presence of 50 $\mu g\,mL^{-1}$ poly(aspartic acid) a) in bulk solution after 5 h, b) in 200 nm membrane pores after 12 h, and c) in 200 nm membrane pores after 5 h.

fairly limited due the small sample volumes used. The EXAFS spectra of the samples, together with the corresponding Fourier transforms and the calculated fits are shown in Figure SI6, while the best fit parameters are summarized in Table SI1. The spectra from the nanorods isolated after 5 h could only be fitted with one shell, comprising 6 oxygen scatterers at 2.38 Å, which is comparable to both calcite and vaterite structures.[20] More structural information could be obtained from the partially crystalline samples, and a superior fit was achieved using two shells as compared with one. The 12 h nanorod samples exhibited short-range structures comprising shells of 6 O and 6 Ca at 2.35 Å and 4.01 Å, respectively, while shells of 6 O and 6 Ca at 2.38 Å and 4.18 Å were determined for the 5 h control sample. In both cases the data analysis shows clear evidence for the second shell. The Ca–Ca distance is rather characteristic for the $CaCO_3$ polymorphs and reveals that the 12 h nanorod sample has short-range order indicative of calcite (where the Ca–Ca distance is 4.06 Å), while the value for the 5 h control sample is comparable with the Ca–Ca distance of 4.21 Å in vaterite.[20] The data is therefore consistent with the observed formation of calcite nanorods in the membrane pores, and the fact that PILP crystallizes in bulk solution to give films which are a mixture of vaterite and calcite. Indeed, this suggests that vaterite may act as a significant precursor to calcite in the crystallization of PILP, which is in perfect correspondence with our previous findings.[20]

That the $CaCO_3$ particles produced from the PILP phase are so distinct in aspect ratio and yield from those produced by the other methods suggests that they must form by a different mechanism. Particle formation through ion-by-ion growth or from ACC in the absence of additives occurs by conventional diffusion of ions or precursor ACC particles into the membrane pores. This is supported by the experimental data, where the size of particles varies according to the

reaction time, and intra-membrane rods were invariably shorter than the membrane thickness of 10–15 μm. This effect is even more pronounced in the smaller 50 nm pores and can be attributed to a growing $CaCO_3$ particle blocking of the pore width, thereby preventing further counter-diffusion of ions and restricting ion-flow to a single direction. Further, previous work with larger pores has shown that in the absence of additives, ACC particles ca. 0.1 μm in size coat the internal surface of the membrane pore before filling in the volume.[10,11] This particle size alone prevents this mechanism from operating in pores as small as 50 nm, such that the ACC is likely to form directly in the pore and be limited by ion diffusion.

Particle formation from the PILP phase, in contrast, is characterized by a number of features which immediately suggests a mechanism analogous to the uptake of a liquid into a pore by capillarity. In the first place, the PILP phase infiltrates highly effectively into membrane pores of very high aspect ratio, rapidly filling their entire volume. Secondly, while the yield of particles is lower at earlier growth times, they all exhibit identical high aspect ratios. Capillarity,[22] or the imbibition of liquid by pores, arises due to the pressure drop across the curved interface of liquid in a pore. In a classic configuration, liquid rises in an open, vertical tube until the lower pressure on the liquid side of the liquid–vapor interface plus the hydrostatic pressure at the bottom of the liquid column equals the pressure on the vapor side of the interface. Thus, any fluid that wets the walls of a pore will be drawn into it by a pressure that is inversely proportional to the pore radius, and the movement of the interface will continue indefinitely unless balanced by gravity; a horizontal pore can therefore fill completely. Capillarity is also not restricted to a liquid/vapor system but occurs just as readily by displacement of a second, incompletely miscible liquid.

A schematic diagram showing the uptake of PILP into an open pore and a pore sealed at one end is shown in Figure 4. The possible operation of capillary action in the current system was investigated by repeating the experiment with a membrane where one side was coated to block the pores at one end only. Particle growth under these conditions was limited, with small rods with aspect ratios of only 5–10 being produced in the 50 nm pores (Figure 4b). This provides strong evidence for capillarity as only limited imbibition can occur under these conditions, particularly in the case of two incompressible fluids. Further, in larger 200 nm membrane pores which had been sealed at one end, less pronounced imbibition was observed, such that the mineral only sealed the open end while coating the pore walls further in (Figure 4c). Therefore, at the time of partial imbibition, there was an interface between the solution (now void space) and the PILP (now solid). These observations therefore confirm previous ideas about the uptake of PILP into pores by capillary action[17,23] and show that the fluid-like phase wets the pore walls in preference to the solution. Further, they are also consistent with the PILP "droplets" forming by a microphase separation due to the interaction of the negatively charged polyelectrolyte and carbonate ions, with the positively charged calcium ions.[24,25] As a characteristic feature, these droplets exhibit low charge[26] and can therefore readily

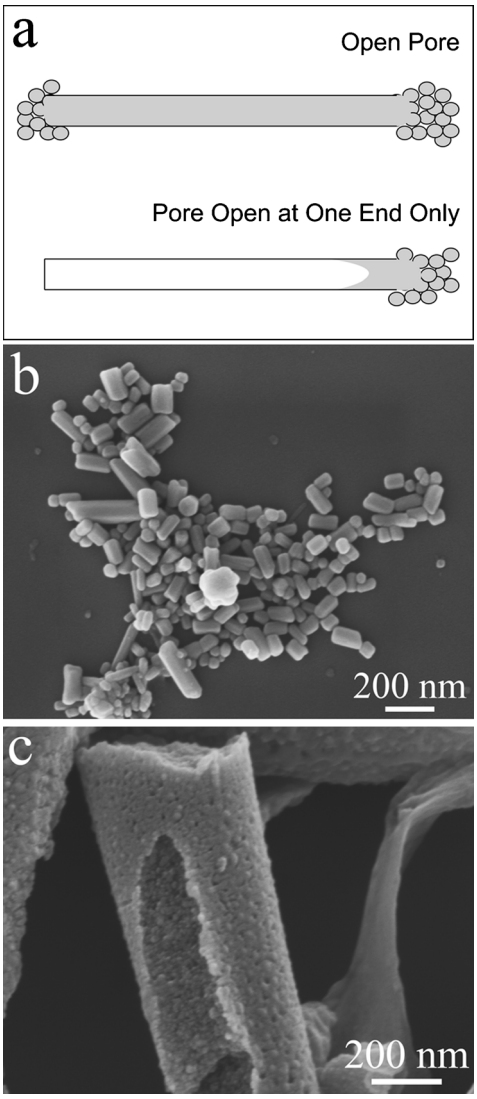

Figure 4. a) Schematic diagram of the uptake of PILP into an open pore, and a pore sealed at one end only. b,c) $CaCO_3$ crystals precipitated in membrane pores when one side of the membrane is blocked, with pore sizes of b) 50 nm and c) 200 nm.

condense within the membrane pore. It is also interesting to note that the uptake of polyelectrolyte-stabilized particles into capillaries has previously been described as the process of "lumen loading" in papermaking. Lumen loading involves the introduction of filler particles such as titania, calcite, or magnetite into the interior of cellulose fibers, and the efficiency of the process is known to be greatly enhanced by the addition of polyelectrolytes.[27–29]

After filling the membrane pore with PILP/ACC its crystallization is accompanied by a loss of water, which leads to a reduction in the volume of the mineral phase. An estimate of this volume change can be made considering that the density and molar volumes of ACC with composition $CaCO_3{\cdot}H_2O$ are 1.62 $g\,cm^{-3}$ and 73 cm^3, respectively,[30] while those of calcite are 2.75 $g\,cm^{-3}$ and 36 cm^3, respectively.[30] The molar volume of water is 18 cm^3. The combined volume of the calcite and expelled water is therefore less than that of the

precursor ACC phase and there is no problem accommodating the expelled water. We also suggest that water loss primarily occurs by transfer to the membrane walls rather than to the ends of the particle. The ACC precursor particles have extremely high aspect ratios, and the distance over which the water must diffuse to escape the mineral phase is much less across the particle width as compared with the length. The particle width would therefore be expected to experience a much larger percentage decrease on crystallization than the length. As a rough estimate, if the rod length is assumed to remain constant (for simplicity), crystallization of $CaCO_3{\cdot}H_2O$ causes a volume contraction of the entire system of 26%, which corresponds to a 12% change in the rod diameter. The solid phase, in contrast, experiences a volume contraction of 50% and a 30% reduction in diameter. While we have used SEM to study the particles in the membranes after crystallization, it is really impossible to state by looking at the ends of the particles alone, that the particles are smaller in width than the pores. Notably, however, no significant change in the length of the intra-membrane particles is observed on crystallization.

That crystallization of an ACC particle with such a high aspect ratio generates a single crystal of calcite as a product is also at first sight surprising and suggests that crystallization is nucleation-limited, such that when nucleation takes place it does so at a single site. Crystallization then progresses from this point in the absence of further nucleation events. Alternatively, a competitive crystal growth mechanism could also be envisaged where, although multiple nucleation sites are present, a dominant crystallite grows at the expense of smaller ones, ultimately yielding a single crystal. Such a mechanism has been observed during the crystallization of ACC in association with Langmuir monolayers.[31]

In discussing the mechanism of formation of these calcite single crystals, it is also interesting to contrast this with previous reports of the formation of $CaCO_3$ fibers and nanowires.[5,7,12–16] In all these cases, fibers were formed in bulk solution either in microemulsions or in the presence of carboxylate-rich soluble additives, and many were considered to form through the aggregation of precursor particles,[12] thereby generating a "mesocrystal" product. Evidence has also been presented that PAA/PAsp may promote fiber formation through a growth mechanism analogous to the vapor–liquid–solid (VLS) and solution–liquid–solid (SLS) processes responsible for the catalytic formation of nanowires.[5,12] Notably, bundles of nanowires of $CaCO_3$ with convoluted morphologies and extremely high aspect ratios were precipitated within reverse micelles of Triton-X[14] and rod-shaped calcite single crystals were formed in cetyl trimethylammonium bromide (CTAB) microemulsions,[13] and in the presence of an 90/10 acrylic acid/styrene copolymer.[15] Poly(acrylic acid) and its analogue poly(aspartic acid) are also particularly effective in promoting fiber formation.[5,7,12]

The results presented here therefore clearly show that crystallizing ACC within a confined reaction volume provides an effective route for controlling ACC crystallization, and that crystals with remarkable structures may form. Given that the pores employed are many orders of magnitude larger than the volume at which changes in the thermodynamic stabilities of the $CaCO_3$ polymorphs would be observed,[4] this effect is attributed to changes in the kinetics of the ACC crystallization. Our data demonstrate that ACC crystallization proceeds more slowly in the membrane pores than in bulk solution, which we suggest is due to the limited contact of the intra-membrane ACC particle with the bulk solution. Indeed, there is strong evidence from biogenic systems that dehydration of ACC precedes its crystallization, even in aqueous environments,[32] and it is possible that water loss may be retarded in the dry environment of the membrane pores, thereby slowing crystallization. This reduced crystallization rate, in combination with the confined environment of the ACC precursor particle in the membrane pore then either limits the number of nuclei formed within the ACC phase, or facilitates the operation of a competitive growth mechanism among multiple nuclei, which leads to a single-crystal product.

In this vein, it is interesting to note that formation of the sea urchin larval spicule—which is a single crystal of calcite with tri-radiate form—takes place on crystallization of a transient ACC phase within a membrane-bound compartment.[33] This occurs in the absence of bulk water with the membrane in contact with the spicule surface, suggesting that exclusion of water from the crystallization environment may provide organisms with a mechanism for controlling ACC crystallization.[34] Our system, in which a single ACC precursor particle transforms to give a calcite single crystal of identical size and shape, therefore provides a unique opportunity for understanding the mechanism by which ACC crystallizes to single-crystal products, as occurs biologically. It is envisaged that this synthetic approach could be applied to a wide range of materials which can be precipitated through amorphous precursor phases, leading to single crystals with unusual morphologies.

Experimental Section

A full description of the experimental methods is provided in the Supporting Information. Briefly, calcium carbonate was precipitated within the 50 nm and 200 nm pores of polycarbonate track-etch (TE) membranes (Isopore, Millipore) using three protocols: at room temperature in the absence of additives (no ACC precipitated), at low temperature in the absence of additives (ACC precipitated), and at room temperature in the presence of the additive poly(acrylic acid) (PAA) or poly(aspartic acid) (PAsp) (a PILP phase is produced which subsequently transforms to ACC). In addition, two experimental setups were employed, such that $CaCO_3$ was precipitated either using double diffusion, or through ammonium carbonate diffusion. Use of these contrasting methods gave superior filling of the membrane pores according to the calcium carbonate precipitation protocol employed. The $CaCO_3$ particles were analyzed by using a range of techniques: scanning electron microscopy (SEM), transmission electron microscopy (TEM), high resolution TEM (HRTEM), Raman microscopy and IR spectroscopy. Selected samples were also analyzed by using X-ray absorption spectroscopy (XAS).

Received: June 25, 2011
Revised: August 2, 2011
Published online: November 8, 2011

Keywords: amorphous calcium carbonate · biomineralization · calcite · nanorods · nanowires

[1] L. B. Gower, *Chem. Rev.* **2008**, *108*, 4551.
[2] L. Addadi, S. Raz, S. Weiner, *Adv. Mater.* **2003**, *15*, 959.
[3] F. C. Meldrum, H. Cölfen, *Chem. Rev.* **2008**, *108*, 4332.
[4] C. J. Stephens, S. F. Ladden, F. C. Meldrum, H. K. Christenson, *Adv. Funct. Mater.* **2010**, *20*, 2108.
[5] M. J. Olszta, S. Gajjeraman, M. Kaufman, L. B. Gower, *Chem. Mater.* **2004**, *16*, 2355.
[6] N. Sommerdijk, E. N. M. van Leeuwen, M. R. J. Vos, J. A. Jansen, *CrystEngComm* **2007**, *9*, 1209.
[7] S. Kumar, T. Ito, Y. Yanagihara, Y. Oaki, T. Nishimura, T. Kato, *CrystEngComm* **2010**, *12*, 2021.
[8] A. S. Finnemore, M. R. J. Scherer, R. Langford, S. Mahajan, S. Ludwigs, F. C. Meldrum, U. Steiner, *Adv. Mater.* **2009**, *21*, 3928.
[9] J. Aizenberg, D. A. Muller, J. L. Grazul, D. R. Hamann, *Science* **2003**, *299*, 1205.
[10] E. Loste, F. C. Meldrum, *Chem. Commun.* **2001**, 901.
[11] E. Loste, R. J. Park, J. Warren, F. C. Meldrum, *Adv. Funct. Mater.* **2004**, *14*, 1211.
[12] J. H. Zhu, J. M. Song, S. H. Yu, W. Q. Zhang, J. X. Shi, *CrystEngComm* **2009**, *11*, 539.
[13] D. X. Liu, M. Z. Yates, *Langmuir* **2006**, *22*, 5566.
[14] D. B. Kuang, A. W. Xu, Y. P. Fang, H. D. Ou, H. Q. Liu, *J. Cryst. Growth* **2002**, *244*, 379.
[15] L. Moore, J. D. Hopwood, R. J. Davey, *J. Cryst. Growth* **2004**, *261*, 93.
[16] Y. Y. Kim, A. N. Kulak, Y. T. Li, T. Batten, M. Kuball, S. P. Armes, F. C. Meldrum, *J. Mater. Chem.* **2009**, *19*, 387.
[17] M. J. Olszta, E. P. Douglas, L. B. Gower in *Materials Inspired by Biology, Vol. 774* (Eds.: J. L. Thomas, K. L. Kiick, L. A. Gower), Materials Research Society, Warrendale, **2003**, p. 127.
[18] D. B. Williams, C. B. Carter, *Transmission Electron Microscopy*, Springer, New York, **2009**.
[19] Y. Levi-Kalisman, S. Raz, S. Weiner, L. Addadi, I. Sagi, *Adv. Funct. Mater.* **2002**, *12*, 43.
[20] R. S. K. Lam, J. M. Charnock, A. Lennie, F. C. Meldrum, *CrystEngComm* **2007**, *9*, 1226.
[21] Y. Politi, Y. Levi-Kalisman, S. Raz, F. Wilt, L. Addadi, S. Weiner, I. Sagi, *Adv. Funct. Mater.* **2006**, *16*, 1289.
[22] A. Einstein, *Ann. Phys.* **1901**, *309*, 513.
[23] M. J. Olszta, E. P. Douglas, L. B. Gower, *Calc. Tissue Int.* **2003**, *72*, 583.
[24] A. Ikegami, N. Imai, *J. Polymer Sci.* **1962**, *56*, 133.
[25] M. A. V. Axelos, M. M. Mestdagh, J. Francois, *Macromolecules* **1994**, *27*, 6594.
[26] B. J. McKenna, J. H. Waite, G. D. Stucky, *Cryst. Growth Des.* **2009**, *9*, 4335.
[27] S. Zakaria, B. H. Ong, S. H. Ahmad, M. Abdullah, T. Yamauchi, *Mater. Chem. Phys.* **2005**, *89*, 216.
[28] A. T. Horvath, A. E. Horvath, T. Lindstrom, L. Wagberg, *Langmuir* **2008**, *24*, 10797.
[29] J. Petlicki, T. G. M. van de Ven, *Colloids Surf. A* **1994**, *83*, 9.
[30] J. Bolze, B. Peng, N. Dingenouts, P. Panine, T. Narayanan, M. Ballauff, *Langmuir* **2002**, *18*, 8364.
[31] E. M. Pouget, P. H. H. Bomans, J. Goos, P. M. Frederik, G. de With, N. Sommerdijk, *Science* **2009**, *323*, 1455.
[32] Y. Politi, R. A. Metzler, M. Abrecht, B. Gilbert, F. H. Wilt, I. Sagi, L. Addadi, S. Weiner, P. Gilbert, *Proc. Natl. Acad. Sci. USA* **2008**, *105*, 17362.
[33] E. Beniash, J. Aizenberg, L. Addadi, S. Weiner, *Proc. R. Soc. London Ser. B* **1997**, *264*, 461.
[34] E. Beniash, L. Addadi, S. Weiner, *J. Struct. Biol.* **1999**, *125*, 50.

